Warped-Compression: Enabling Power Efficient GPUs through Register Compression

Sangpil Lee[†]   Keunsoo Kim[†]   Gunjae Koo[‡]   Hyeran Jeon[‡]   Won Woo Ro[†]   Murali Annavaram[‡]

[†]Yonsei University   [‡]University of Southern California

{madfish,keunsoo.kim,wro}@yonsei.ac.kr   {gunjae.koo,hyeranje,annavara}@usc.edu

Abstract

This paper presents Warped-Compression, a warp-level register compression scheme for reducing GPU power consumption. This work is motivated by the observation that the register values of threads within the same warp are similar, namely the arithmetic differences between two successive thread registers is small. Removing data redundancy of register values through register compression reduces the effective register width, thereby enabling power reduction opportunities. GPU register files are huge as they are necessary to keep concurrent execution contexts and to enable fast context switching. As a result register file consumes a large fraction of the total GPU chip power. GPU design trends show that the register file size will continue to increase to enable even more thread level parallelism. To reduce register file data redundancy warped-compression uses low-cost and implementation-efficient base-delta-immediate (BDI) compression scheme, that takes advantage of banked register file organization used in GPUs. Since threads within a warp write values with strong similarity, BDI can quickly compress and decompress by selecting either a single register, or one of the register banks, as the primary base and then computing delta values of all the other registers, or banks. Warped-compression can be used to reduce both dynamic and leakage power. By compressing register values, each warp-level register access activates fewer register banks, which leads to reduction in dynamic power. When fewer banks are used to store the register content, leakage power can be reduced by power gating the unused banks. Evaluation results show that register compression saves 25% of the total register file power consumption.

1. Introduction

GPUs are designed as throughput-oriented processors, which rely on massive thread-level parallelism (TLP) to improve computational throughput. Compared to multi-threaded CPUs that support only a few hardware thread contexts, GPUs maintain hundreds or even thousands of active threads. To effectively manage massive number of threads, a set of threads are grouped into a warp (also called wavefront). All threads in a warp execute instructions in lock-step, which is called single-instruction multiple-thread (SIMT) execution model [3]. GPU evolution over generations has shown that the number of execution units has been steadily increasing. To fully utilize the execution units, the number of concurrent thread contexts has also increased [8, 7, 6].

To enable fast context switch between threads, GPUs maintain all active thread contexts in a large register file. The size of the register file in GPUs is much larger than that of CPUs. For instance, the NVIDIA Maxwell GPU has 64K 32-bit registers per each streaming multiprocessor (SM) [6], which is much larger compared to 336 physical registers per core on Intel Haswell CPU [26].

Given their huge size, register file contributes up to 15% of the total GPU chip power even in older generation GPUs [35, 36]. There have been two approaches to save register file power consumption. The first approach turns off unused part of the register file to save both leakage and dynamic power, and places used registers in drowsy state to reduce leakage power. This approach exploits the observation that some applications utilize only a fraction of the entire register file or have large register inter-access time [9]. The second approach to optimize dynamic power is based on the register use locality. For instance, register file cache [21] uses a small cache to capture register access locality thereby reducing frequent accesses to the large register file banks. In [50], the authors proposed a register file hierarchy to store a small subset of registers in an SRAM while a lower power DRAM stores the larger register file content.

This paper explores and exploits a different property of register files, namely value similarity. In the SIMT execution model since all threads within a warp execute the same instruction, access to register file is also performed at warp granularity. Because a warp consists of dozens of threads that are identified using consecutive thread indices, many GPU programming approaches use thread index to access and manipulate data. As such many computations that rely on thread index also operate on register data that exhibit strong value similarity. Note that throughout this work we use the simple

metric of arithmetic distance to measure value similarity. An arithmetic distance of n indicates that two values differ by $|n|$. Even though register values across threads in a warp are similar each thread register stores the entire redundant value. Repeatedly storing, reading, and writing redundant data is one source of power inefficiency that this work addresses.

Prior works [16, 17, 30, 33] have also used the notion of value similarity. The authors in [16] defined the notion of value structure to capture scenarios where different threads within a warp execute on input operands that can be described as a simple function of thread ID and block ID. Value structure can then be exploited for improving memory storage efficiency [17]. The authors in [30] exploited this value structure further to create a separate affine functional unit that performs more power efficient computations when a warp instruction exhibits value structure. They also proposed hardware support for branch instruction execution in the presence of value structure to reduce the cost of branch resolution latency.

Inspired by these prior studies, this paper takes an orthogonal approach to exploit value similarity to improve register file power consumption. It proposes warped-compression, a compression scheme for GPU register files based on the similarity of register values. Compression enables both dynamic and leakage power reduction. Dynamic power is reduced by decreasing the access count to each register bank by compressing the operand data into fewer physical register banks. Furthermore, dynamic power is reduced because the compressed register read and write operations activate fewer bitlines in the register file and fewer bits are moved across the wires between register file and execution unit where the data is processed. As has been shown in several studies [29, 18, 31, 42], data movement is as power hungry as computation. For instance in [29] the authors showed that moving three 64-bit inputs operand from registers to execution unit burns as much energy as doing a double precision floating point operation. Leakage power also can be reduced when using a narrow width banked register file organization as is the case with GPUs. When a wide register can be compressed to be stored in fewer register banks, there are opportunities to power gate an entire register bank.

We summarize the contributions of the paper as follows.

- We characterize value similarity of the registers at the granularity of a warp access. Our findings show that threads within a warp read and write values with small arithmetic difference, particularly when the warp is in a non-divergent code section, but the value similarity drops under branch divergence.
- We provide a detailed design of warped-compression that uses low-cost and implementation-efficient base-delta-immediate (BDI) compression scheme [40], and takes advantage of banked register file organization used in GPUs. BDI can quickly compress and decompress a warped register by selecting one of the thread register values as the primary base value and then computing delta values of all other thread registers with respect to the base value.
- We show the power and performance impact of different design configurations exploring various design spaces including compression parameters, access energy, and compression latency.

The rest of this paper is organized as follows. Section 2 provides background on the register file organization of modern GPUs and data compression method. Section 3 presents value similarity characterization for GPU applications. Section 4 describes the compression algorithm design. Section 5 discusses the microarchitecture design to support warped-compression including further optimizations on the BDI algorithm. Section 6 presents the evaluation methodology and results. Section 7 discusses related works and Section 8 concludes the paper.

2. Background

2.1. GPU Register File

GPUs are designed to maximize computation throughput using massive thread parallelism, rather than optimizing just the per-thread computation latency. The key components of modern GPUs are a large number of execution units and its ability to maintain multiple threads in flight to feed the execution units. For instance, NVIDIA Kepler GPUs have 192 execution units, 2048 in-flight threads, and 256 KB register file per processing core called streaming multiprocessor (SM) [8].

GPUs adopt SIMT model to efficiently organize the execution of a large number of threads. In the SIMT model, the basic unit of execution is a thread bundle of tens of threads. The thread bundle is called a warp (CUDA of NVIDIA [3]) or a wavefront (OpenCL [4]), whose size is 32 and 64 threads, respectively. In this paper, we use the notion of warp following the CUDA terminology although the technique itself is independent of this choice. All 32 threads in a warp execute the same instruction. Therefore, to execute an integer or floating point warp instruction that has 32 threads, the register file needs to supply 32 × (number of source operands) register values to the SIMT execution units. In this paper, we use the term *register* or *warp register* for an architectural register accessed by a warp instruction, and *thread register* to specifically indicate the register associated with each thread within a warp.

To provide large bandwidth without unduly increasing complexity, GPU register file is constructed with multiple SRAM banks as shown in Figure 1. The baseline register file design has all the components shown in the figure except for the two highlighted boxes, named compressor unit and decompressor unit. The two new boxes will be described later when we present our modified register file design. For the baseline register design, we assume a 128 KB register file per each SM made up of 32 banks (4 KB registers per bank). Each bank has one read and one write port, and each entry in a register bank is 128-bit wide, and there are 256 entries per bank. In
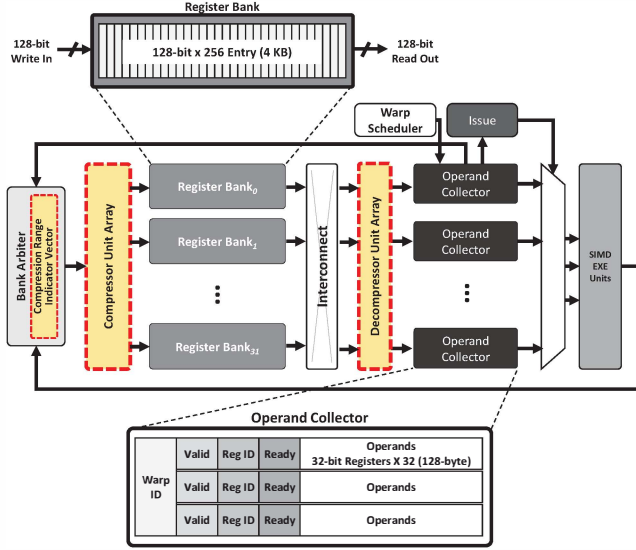
Figure 1: Base GPU register file design with proposed enhancements for compression

this configuration, each register bank entry can store up to four 32-bit register values. All thread registers in a warp are statically allocated on consecutive banks with the same entry index. Therefore, to read one operand of a warp instruction, a buffering unit called operand collector needs to access up to eight register banks with the same index within each bank. While operands from different banks may be concurrently read, operands that access the same bank lead to bank conflicts. To effectively handle operand fetch latency, the operand collector assembles operand values from multiple SRAM banks. This register file organization is very close to the register file design description provided for the NVIDIA Fermi architecture [7] and has also been used in several prior studies [27, 20, 21, 22]. In spite of significant design effort to optimize the power of GPU register file, it consumes 15% of the GPU's total power, and it is the second largest function block behind execution units [35, 36].

2.2. Data Compression for Cache and Memory

GPUs are already bandwidth constrained when it comes to main memory usage. To alleviate the bandwidth constraint between GPU and main memory, data compression has already been adopted. State-of-the-art GPUs aggressively adapt graphics data compression techniques such as delta color compression [6, 37]. For instance, NVIDIA Maxwell is supposed to improve the effective main memory bandwidth by 25% using a compression scheme [6].

In the context of CPUs, cache compression at the granularity of a cache line has been studied to increase performance by more efficiently utilizing data caches. Data compression schemes for on-chip memory structures such as caches should satisfy two conditions. First, cache data must be amenable for compression by providing a high compression ratio, which is

defined as the original data size divided by the compressed data size. Second, compression and decompression latency should be sufficiently short in order to avoid performance degradation. Because the compressed cache line stored in the cache must be decompressed before delivering to the pipeline, decompression latency increases cache hit latency. Similarly, cache updates and cache fills may also be delayed since the data may be compressed before storing into the cache. Due to these characteristics, cache compression schemes have focused on L2 or last level cache, which has better latency tolerance than L1 caches [10, 14, 11]. Compression has also been used for instruction cache compression which exhibit high compression ratios [34].

In the context of GPUs, since register files are much larger than caches, compression techniques that target register files can deliver higher return on design investment. Instead of relying on cache compression schemes, the unique aspects of GPU register file organization and value similarity can be exploited to design a highly efficient GPU-specific register file compression mechanism.

3. Similarity of Register Values in GPU

In this section, we analyze the value similarity among the thread registers in a warp for both the divergent and non-divergent warps. We calculate the arithmetic distance between two successive thread registers within a warp register which is written during each benchmark's execution. For instance, if a register $r0$ was written by a warp, then there are 32 thread registers that are written, each corresponding to one thread within that warp. We then compute the arithmetic distance between the first thread register and the second thread register, second thread register and third thread register, and so on. Each arithmetic distance computed is placed into one of four bins. The first bin is the zero distance bin where two successive thread registers are identical. The second bin is called the 128 bin where two successive thread registers that do not fall in the first bin differ by at most $|128|$. The third bin is called the 32K bin where two successive thread registers differ by at most $|2^{15}|$ and do not fall in the second bin. The last bin is called random when the register differences exceed $|2^{15}|$.

Figure 2 categorizes the each register write into four categories based on value similarity at the time the register value was written, across a range of GPU benchmarks (simulation methodology is described later in Section 6.1). For each benchmark, the first bar shows the categorization for instructions when the warp is non-divergent. The second bar shows the categorization for warp instructions that are divergent. Figure 3 shows the ratio of divergent and non-divergent code to show the relative importance of these two execution phases. 79% of the warp executions on average are non-divergent in these benchmarks. As presented in Figure 2, during non-divergent execution phase 79% of the registers are categorized as not random. This data suggests that compressing an entire warp register is very effective in reducing the register file size dur-
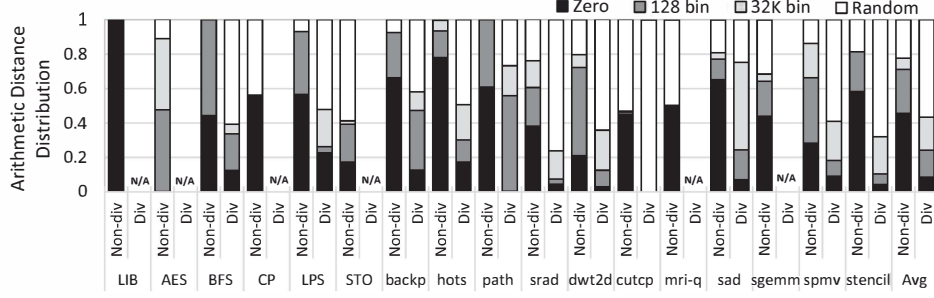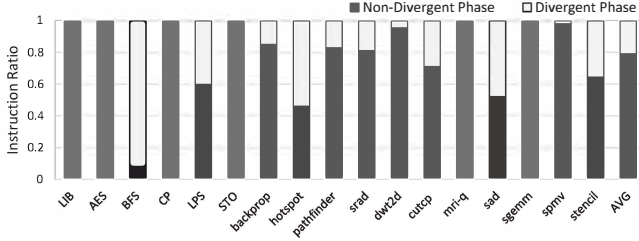
Figure 2: Characterization of register values

Figure 3: Ratio of non-diverged warp instructions

ing 62% (79% of the 79%) of the total execution time. Even during divergent phases there is still a significant amount of value similarity in the register file, although the random data category increases from 21% to 57% during divergence.

We observed two predominant sources of register value similarity. First, many thread-specific local variables are accessed using thread index. Data arrays, for instance, are accessed using thread ID so that each thread computes with data assigned to that thread. Thread IDs of successive threads in a warp differ by one and hence a warp register used to data arrays exhibit strong value similarity. Second, dynamic range of the input data also impacts similarity. Figure 4 shows the kernel code of *pathfinder* (some code sections are omitted for brevity). In this example, some local variables are assigned similar or even the same value across all threads. For instance, *bx* on line 6 is the thread block ID which is fixed for all threads, and *tx* is thread index. Some local variables are computed mostly using constant variables. For instance, *small_block_cols* on line 7 is computed using the *BLOCKSIZE* and *HALO* values, which are both constant values in the kernel, and *iteration*, which is a fixed input parameter value for each invocation of the *pathfinder_kernel*. In addition, the input data arrays for *pathfinder*, namely *prev[]* on line 15 to 17, and *wall[]* on line 21, has a very narrow dynamic range (0 to 9). As a result, registers that hold variables such as *left*, *up*, *right*, *shortest* also exhibit strong value similarity.

Note that a number of previous works have shown that value similarity in CPU applications are frequently observed [40, 51, 45]. In the case of CPUs these similarities are measured across different architected registers. Our results show that strong value similarity persists for threads within a warp even in GPUs. This observation provides a strong motivation to develop the proposed register compression technique.

```
1   #define IN_RANGE(x, min, max)   ((x)>=(min) && (x)<=(max))
2
3   __global__ void pathfinder_kernel(int iteration, ...)
4   {
5           ...
6       int tx=threadIdx.x; int bx = blockIdx.x;
7       int small_block_cols = BLOCKSIZE-iteration*HALO*2;
8       int blkX = small_block_cols*bx-border;
9       int xidx = blkX+tx;
10          ...
11      for (int i=0; i<iteration ; i++){
12          computed = false;
13          if( IN_RANGE(tx, i+1, BLOCKSIZE-i-2) && isValid){
14              computed = true;
15              int left = prev[W];
16              int up = prev[tx];
17              int right = prev[E];
18              int shortest = MIN(left, up);
19              shortest = MIN(shortest, right);
20              int index = cols*(startStep+i)+xidx;
21              result[tx] = shortest + wall[index];
22              ...
23          }
24      }
25              ...
26  }
```

Figure 4: Example of GPU kernel code (*pathfinder*)

4. Compression Algorithm

In order to maintain register values in a compressed state, compression and decompression procedures are needed for every access to the register file. There is a tradeoff between how well the register state can be compressed using complex compression algorithms, such as LZW [38, 19], and the latency of these algorithms which will increase the register access time. We explored a wide range of compression algorithms to measure the compression ratio and their compression latency. Given the motivational data that showed that majority of the register values have a short arithmetic distance, we selected a compression algorithm that can achieve high compression ratios at low latency when compressing values with short arithmetic distance.

We found that base-delta-immediate (BDI) compression algorithm [40] is the most suitable algorithm for GPU register file compression. BDI compression has two parameters: <base value, delta value>. In the BDI algorithm, the data is divided into several chunks, and the value of the first chunk is selected as a *base* value. For all chunks, difference to the base values, which is called the *delta*, is computed by subtraction. Clearly, if the value of the base chunk is similar to the value of other

Table 1: Possible combinations of chunk size

Base Size (B)	Delta Size (B)	Comp. Size (B)	Required # Reg. Banks	Used?
1	0	1	1 (16 B)	N
2	1	65	5 (80 B)	N
4	0	4	1 (16 B)	Y
4	1	35	3 (48 B)	Y
4	2	66	5 (80 B)	Y
8	0	8	1 (16 B)	N
8	1	23	2 (32 B)	N
8	2	38	3 (48 B)	N
8	4	68	5 (80 B)	N

Figure 5: Breakdown of <base, delta> values to achieve best compression ratio

chunks, the delta value is small. This small delta value can then be represented using fewer number of bits than the number of chunk bits. Using single base and the delta values of each chunk, we can recover the original data. Thus BDI compresses the original data into a single base value followed by a series of delta bits. If the base value differs significantly from a given chunk then the delta value may need a large number of bits for its representation, thereby reducing, or even eliminating, opportunities for compression.

The BDI algorithm has very low decompression latency, because decompression is performed by simply adding the base value and the delta value for each chunk. Therefore, this is very suitable where the decompression latency is critical, which is the case for the register file read operation in a GPU pipeline.

The original BDI algorithm as described in [40] repeats the compression process for a wide range of base and delta lengths, such as 2, 4, or 8-byte base and delta lengths, and then selects the values for the two parameters, <base value, delta value>, that provide the maximum compression ratio. While this exploratory approach is acceptable for latency tolerant compression mechanisms, it is inefficient to explore these parameter values at runtime for achieving the highest compression ratio for register files. Such an exploration adds large power and latency overheads.

We mitigate the overheads by allowing only three fixed size representation of the compressed data. If the data cannot be compressed into one of the three sizes then the register is left uncompressed. To select the fixed bit width representation it is useful to consider the register file organization. In GPU register file, the unit of data storage is the width of a bank. As discussed earlier, each register bank is 16-byte wide. Thus there are discrete steps in register bank usage; anytime the compressed data exceeds a 16 byte boundary an extra register bank must be accessed. Therefore, some combination of base, delta values can be eliminated from consideration because they needlessly straddle the bank boundaries.

In the BDI algorithm, the compressed data length L_{comp} can be calculated statically as the function of base length L_{base}, delta length L_Δ, and input data length L_{input}, which is presented in (1).
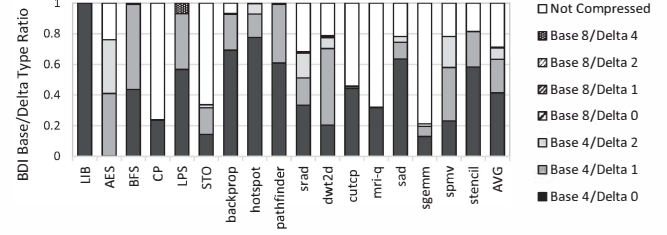
$$L_{comp} = L_{base} + L_\Delta \times (L_{input}/L_{base} - 1) \qquad (1)$$

Table 1 lists the number of 16-byte register banks needed (column titled Required # Reg. Banks) to represent a single 128-byte warp register for a combination of base and delta parameter values. We denote <X,Y> to represent X-byte base size and Y-byte delta size. Consider the <2,1> case; the warp register is first divided into 2-byte chunks (a total of 64 chunks). The first chunk is stored as a two byte value and the remaining 63 chunks are each represented as a 1-byte delta. Thus the total compressed size, if compressed, is 65 bytes; recall that if any 2-byte chunk cannot be compressed to one byte then the entire register will be left uncompressed. The 65-byte compressed representation requires five register banks. On the other hand <4,1> representation requires only three register banks, while <8,1> requires only two register banks. Note that any register that can be compressed with <4,1> can also be compressed with <4,2> since the base size is the same and delta size has been increased to two bytes. Similarly, <8,4> will always compress any register that was compressed with <8,2>, which in turn can compress any register that was compressed with <8,1>. We also included a delta size of zero bytes, which is a special case that can only store register values that falls under the *zero bin* category in Figure 2.

There is a tradeoff between how many registers can be compressed with a given <X,Y> parameter and the number of register banks necessary for representing the compressed register. As a design space exploration study we implemented the original BDI compression scheme that automatically selects the best <X,Y> value based on the compression ratio. Every register write operation was tracked by the BDI compression algorithm and based on the warp register values it selects one of the following set of <X,Y> parameters: <4,0>, <4,1>, <4,2>, <8,0>, <8,1>, <8,2>, <8,4>. On a register write operation the BDI compression algorithm computes the compression ratio with each of the listed parameter settings and then picks the setting that provides the highest compression ratio.

Figure 5 shows how often the algorithm selected a particular <X,Y> parameter value, as a fraction of total register writes. From the figure it is clear that a base value of eight was rarely selected. This result is intuitive because thread register writes are 4-byte granularity writes, and hence it will be unusual to
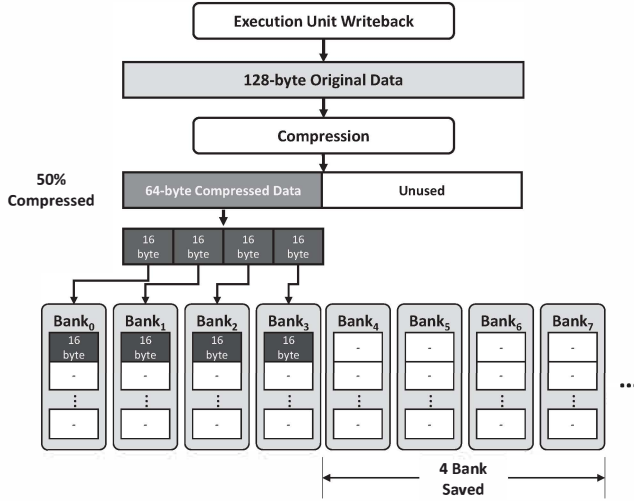
Figure 6: Saving register banks with compression

find no similarity across two single thread registers, but to find similarity across pairs of registers. Based on the data shown in this breakdown we selected <4,0>, <4,1>, <4,2> as the three fixed choices for compressing the data. If the data cannot be compressed using any of the three choices the register will be remain uncompressed. This selection is used as our default implementation in all our results. For this selection each warp register requires a 2-bit compression range indicator, to indicate which of the three compression choices were used to compress the warp register, or if the warp register is left uncompressed. In our implementation, this vector is stored in the bank arbiter, and it is read when a register access is requested, in parallel to bank arbitration.

Note that in our design space exploration studies we evaluated restricting the compression to just one choice amongst <4,0>, <4,1>, and <4,2>. Clearly, selecting a single compression choice reduces decompression complexity but it may also reduce compression capability. Note that <4,0> is quicker to decompress since no delta values need to be added to the base value, but only zero bin category in Figure 2 will benefit from this selection. On the other hand <4,1> improves the reach of the BDI compression algorithm but the decompression latency will increase. We evaluate a range of these tradeoffs in our results sections.

5. Warped-Compression Operation

In this section, we present the detailed operation of warped-compression. Figure 1 shows the block diagram of the warped-compression with the added compression and decompression logic highlighted. When compression is activated, the computed values from the execution units should be compressed before being written to the register file. As illustrated in Figure 6, the compressed register values are split into multiple chunks, each chunk is 16 bytes-wide to fit in one register bank. For instance, if a 128-byte warp operand is compressed to 64-byte with a compression ratio of two, the 64-byte compressed value
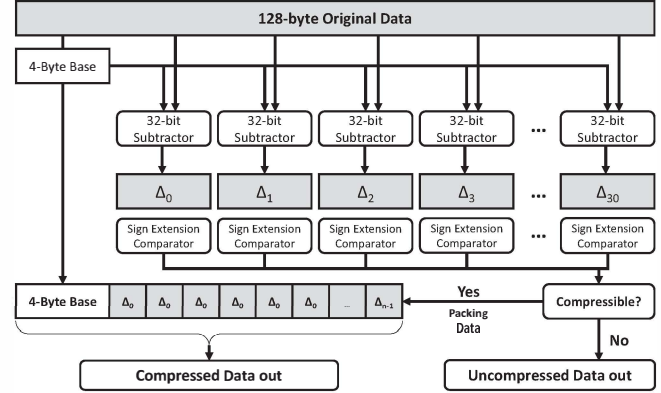

Figure 7: Compressor implementation

is split into four chunks and stored to four consecutive register banks. In this example, compression can halve the number of register banks accessed to store, and later read that register.

As shown in Figure 1 a decompression unit is placed between the execution unit and the register file. The decompression of register values is performed when a register operand of a warp instruction is read from the register file. When a warp instruction is allocated to a collector unit, the operand collector sends access requests for all source operands of the instruction to the bank arbiter. In order to minimize bank conflicts, the arbiter selects access requests that do not access the same bank among the access requests from multiple operand collectors. The arbiter uses the compression range indicator vector to identify whether the register being sourced is in compressed state or otherwise. As described above the two-bit compression range indicator shows the size of the compressed register. Recall that the <4,0> BDI compression stores the entire warp register in a single 16 byte register bank. Similarly <4,1> requires three register bank reads, and <4,2> requires five register bank reads. If the register is in uncompressed state then all eight register banks must be read. When the arbiter accesses a compressed warp register it needs to access only those banks that store the compressed partial chunk of all registers for a warp operand. After all the necessary banks for a compressed operand register are read, the compressed chunks are sent to the decompressor unit and the original 128-byte register value is reconstructed.

5.1. Organization of Compressor

Figure 7 shows the detailed organization of the compressor unit. The compression process is composed of two steps: subtraction and bit comparison. The 128-byte warp register data is divided into 32, 4-byte chunks. Then each chunk is subtracted from the 4-byte base. For implementation simplicity we only use the first chunk of original data as the base value. Sign extension comparators compare sign bits of the subtraction results (deltas) to determine that the subtraction results can be represented using the delta size of either 0, 1 or 2 bytes. Note that this compression process is activated only when the
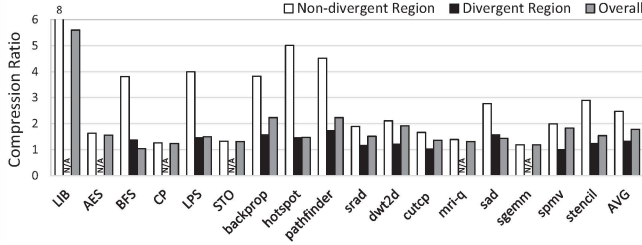
Figure 8: Compression ratio

execution units are writing the data to the register file.

The optimal number of compressor and decompressor units depend on the configuration of register file and execution units. Most warp instructions have two source operands and one destination register. In this case, we need at least two decompression units and one compression unit to process one warp instruction per cycle. Our baseline GPU is capable of executing two instructions per clock and hence in our evaluations we assume the presence of two compressors and four decompressors per SM. As we show, the area overhead of these added blocks is less than 0.3% of the total SM size.

5.2. Handling Branch Divergence

The compression approach described above works well in the absence of branch divergence. As shown earlier, on average 79% of the warp executions are non-divergent. But when a branch divergence occurs, a subset of SIMT lanes of a warp are activated. When the diverged warp instruction completes only the active thread register values must be updated. In the conventional GPU register file, updates to each thread register is controlled by the active mask bit associated with that SIMT lane. Therefore, it is possible to control the updates on a per-thread basis. However, in the presence of compression it is not possible to selectively write a few thread registers into a previously compressed warp register.

Figure 8 shows the compression ratio for divergent and non-divergent regions of the program execution. In order to measure the compression ratio in this figure, we assume that during divergence every new register write will be preceded by a register read operation that first decompresses the data and then allows the active thread values to be updated. The updated register is then compressed again. The figure shows that the compression ratio in the non-divergent region is very high, with an average compression ratio of 2.5. Meanwhile, in the divergent region, the average compression ratio is only 1.3. The low compression ratio implies that applying warp-level register compression is not as effective in the divergent region.

Nonetheless we evaluated different design options to deal with branch divergence considering the cost-benefit tradeoffs of each option. One approach we evaluated is to simply shrink the compression window from a large warp register to a single thread register. In this approach each thread register is individually compressed. However, the compression efficiency is significantly degraded. The basic premise of our work is

inter-thread register value similarity and hence compressing each individual thread register does not exploit inter-thread value similarity.

Another approach is to perform baseline compression even in the presence of divergence. Because BDI compression is performed using all 32 registers in a warp, the destination register for a warp instruction is read first into a temporary buffer and any access requests to the buffered register are simply delayed. Then all active thread registers in the diverged warp write into that buffer. The entire warp register is now current and it is then compressed and stored into the register file. This approach however requires intermediate buffers to store the registers written during divergence, thereby adding area and power overheads.

Based on the data shown in Figure 8, warped-compression relies on a simpler solution – all registers written when executing divergent warp instructions are written to the register file in uncompressed form. But there is still a need to handle the case where the destination register of a divergent instruction is already in compressed state. When the bank arbiter in the register access stage detects a diverged warp instruction that is going to update a compressed destination operand register, a decompression instruction is injected to the execution pipeline. The arbiter simply issues a dummy MOV instruction where the source and destination registers are the same and schedules it ahead of the divergent instruction. The MOV instruction reads and decompresses all 32 registers of the destination operand, and updates uncompressed values to the register file.

We modeled the contention caused by MOV on the register read ports and operand collector buffer in our results, and we observed that the impact of extra contention caused by the MOV instruction was negligible. Note that the MOV instruction is inserted into the execution only when a compressed register is being updated for the first time within a divergent phase. It turns out that during divergence only a few unique registers are updated, compared to the total number of avail-
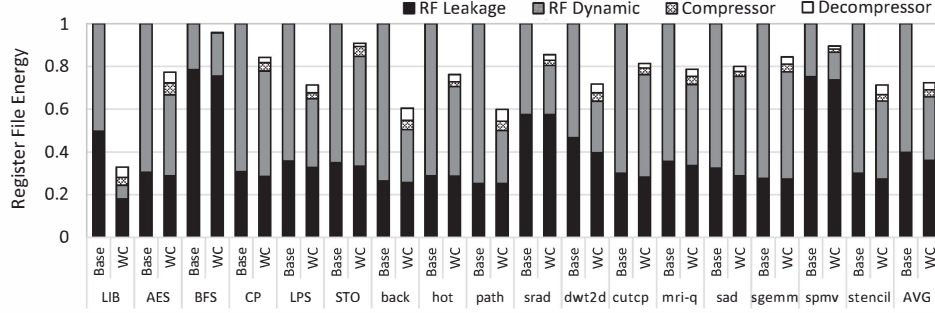
Figure 9: Register file energy consumption

Table 3: Estimated energy and power values (@45nm)

Description	Value
Operating Voltage (V)	1.0
Wire Capacitance (fF/mm)	300
Wire Energy (128-bit, pJ/mm)	9.6
Access energy/bank (pJ)	7
Leakage power/bank (mW)	5.8
Compression unit energy/activation (pJ)	23
Compression unit leakage power (mW)	0.12
Decompression unit energy/activation (pJ)	21
Decompression unit leakage power (mW)	0.08

Figure 10: Portion of power-gated cycles for each bank

able registers. Hence, the number of MOV instructions is only a small fraction of the total instruction count. All these observations are quantified in detail in our results section.

5.3. Support for Reducing Leakage Energy

Apart from reducing dynamic energy by reducing bank accesses, warped-compression can also reduce leakage energy. To minimize leakage, warped-compression applies bank-level power gating techniques for register banks that were left idle after compression. When all the entries in a register bank are not used, the bank is turned off to save leakage power. To enable power gating each register bank is augmented with a sleep transistor to control the bank power delivery, and each register entry in a bank has a valid bit. When all the valid bits are reset the corresponding bank is power gated and when a single entry is needed then that bank is woken up after a wakeup delay, which was set to 10 cycles by default.

6. Evaluation

6.1. Methodology

We modified GPGPU-Sim [12] for detailed simulation of the banked register file design, and modeled additional pipeline stages for both the compression and decompression of the register file. We also modeled the additional read port and operand collector contention due to dummy MOV instructions to handle branch divergence. Detailed GPU microarchitectural parameters are listed in Table 2. We assume that each SM has 4 decompressors and 2 compressors to process 2 warp instructions per cycle from 2 warp schedulers. In order to model overheads with bank-level power gating, we assume 10
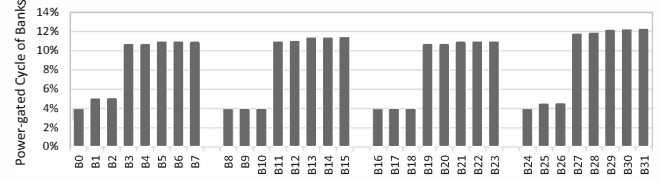
cycles are required to wake up a power-gated register bank. We executed a wide range of benchmark applications from Rodinia [13], Parboil [5], and GPGPU-sim [12].

Table 3 summarizes the estimated energy and power values for register and compression components. CACTI [1] was used to model the access energy and leakage power of a 128-bit wide 4 KB SRAM bank. Wire energy for data transmission was also modeled since the warped-compression reduces the wire movement energy, which contributes to a significant fraction of the total access energy per bank [29, 18, 31, 42]. Wire energy was modeled using a similar methodology presented in previous works [31, 21]. For measuring the wire energy, as presented in Table 3, we assume the wire capacitance of 300 fF/mm and the data read from the register banks travels 1 mm [21]. We also assume 50% of wires move zeros while the other 50% of the wires move ones.

The compression and decompression units are essentially a collection of 32 adder/subtractor modules. The activation energy of the adders is estimated by using the 32-bit adder energy number from recent literature [47]. The other parts of the units, such as comparators with the base value and delta storage circuits, are modeled in RTL level and synthesized with 45nm FreePDK library [2]. Based on the die photo of GF100, the size of an SM is estimated to be 22 mm^2. The estimated area of 2 compressors and 4 decompressors is 0.07 mm^2, which increase the area of an SM by 0.3%.

These power and energy values were used to compute the baseline energy savings. Since these modeled energy values (e.g., wire activity, activation energy of compression/decompression unit) are implementation dependent, to provide robust results we also explored a range of energy expenditures for the wires and the compression/decompression logic blocks in our design space exploration results.
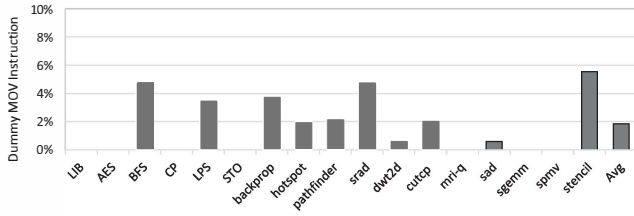
Figure 11: Portion of dummy MOV instructions

Figure 12: Portion of compressed registers

6.2. Energy Reduction

Figure 9 shows the total energy consumed in the register file. For each benchmark we report two stacked bars. The first stacked bar shows the baseline leakage and dynamic energy consumption as a fraction of the total register file energy without any compression capability. The second stacked bar shows warped-compression energy broken into four categories of energy expenditure as a fraction of the total energy consumed in the baseline without any compression. The two new categories are the energy consumed due to compression and decompression. The total energy consumption of warped-compression is significantly less than the baseline, even after accounting for the overhead of the compression and decompression process. Referring to the compression ratio data presented in Figure 8, benchmarks that have high compression ratios are the ones that benefit most from our approach. The number of physical register banks required to store the logical registers decrease in proportion to the compression ratio. Therefore, warped-compression reduces the dynamic energy by reducing bank accesses to the register file. As discussed in Section 3, the dynamic range of the input value strongly affects the value similarity. In case of *LIB*, the input data is initialized to constant values, therefore it has zero dynamic range. As a result, most of warp registers can be perfectly compressed and the register file energy consumption for *LIB* is significantly reduced. Note that leakage energy was also reduced by the bank-level power-gating technique, although leakage energy savings are lower. The average dynamic and leakage energy consumption reduced by 35% and 10%, respectively, which resulted in 25% overall register file energy reduction.

Figure 10 shows the average ratio of power-gated cycles for 32 register banks. We present the average values per bank for all benchmarks. Baseline register file does not have any bank-level power-gating opportunity because all registers are distributed across all banks to prevent bank conflict. On the contrary, warped-compression reduces the number of banks for storing register data, therefore some banks do not contain valid register data and can be power-gated safely. Recall that a warp register is allocated to eight consecutive register banks and as such we show the per bank gating data for four clusters of eight consecutive banks. Since the compressed register data is stored starting from the lowest bank index the fraction of cycles where a bank is power gated increases as we move towards higher bank index in each cluster.
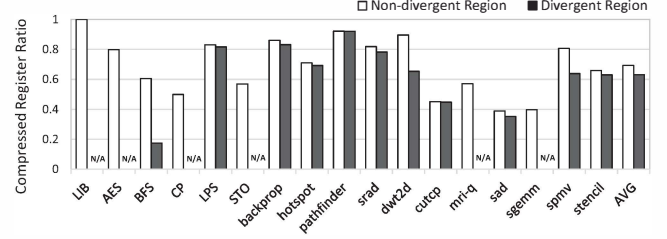
6.3. Impact of Branch Divergence

As discussed in our implementation section any register updated during branch divergence will be first uncompressed using a dummy MOV instruction. Figure 11 shows the number of MOV instructions executed as a fraction of the total instruction count. MOV instructions account for less 2% of the total instruction count. There are two reasons for the small instruction overhead. First, only 21% of the instructions on average diverge across all benchmarks. Second, even during the divergence only the first update to a compressed register results in the MOV operation. The number of registers that were in compressed state during divergent and non-divergent phases of each benchmark are shown in Figure 12. For each benchmark we show as a fraction of the total registers allocated to the application how many registers were in compressed state during the non-divergent (first bar) and divergent (second bar) phases. Note that benchmarks, such as *AES*, do not diverge at all and hence the divergent region bars are marked as N/A. Only a few benchmarks, *BFS*, *dwt2d* and *spmv*, show greater than 10% reduction in the number of compressed registers during divergent code. These benchmarks lose some opportunities for compression due to our implementation choice. For the remaining benchmarks the number of compressed registers stay almost the same both during divergent and non-divergent regions. While computing the average for divergent region we removed all those benchmarks that exhibit zero divergence. Since we disable compression during divergence and yet it reduces the compressed register ratio by 63% we can conclude that only a few registers were decompressed during divergent phase.

6.4. Impact on Execution Time

The proposed register compression may negatively impact execution time in two ways. The first reason is the additional pipeline stages to compress and decompress register values. The second reason is the increased number of dummy MOV instructions when handling branch divergence. Figure 13 shows the performance impact due to compression. As we already showed earlier the number of additional dummy MOV instructions is negligible. Hence, most latency increase seen can be attributed to the increased pipeline depth. But compared to the baseline, the average performance loss is only 0.1%, and in most cases the performance is unchanged.
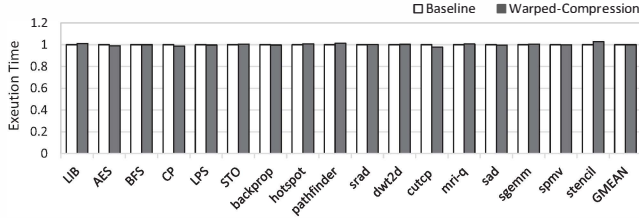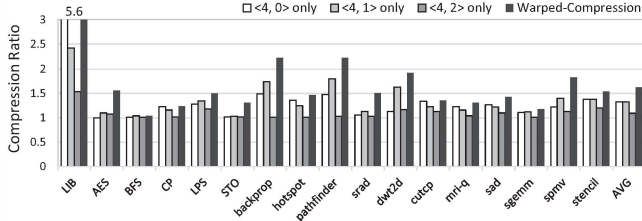
Figure 13: Impact on execution time

Figure 14: Energy reduction: GTO and LRR warp schedulers

Figure 15: Compression ratio for various compression parameters

Figure 16: Energy consumption for various compression parameters

6.5. Impact of Warp Scheduling

Warp scheduling does not change compression ratio but it may impact how compressed registers from different warps may coexist thereby changing the number of idle banks that may be power gated. As shown in Table 2, our baseline configuration uses Greedy-Then-Oldest (GTO) as a default warp scheduler. To quantify the sensitivity of our results to warp scheduler, we replaced GTO with Loose Round-Robin (LRR) scheduler [41]. The GTO scheduling algorithm runs a warp until the warp stalls then switches the oldest ready warp, whereas the LRR scheduling switches warps in every scheduling cycle in round-robin order, as long as there is a waiting ready warp. Figure 14 shows register energy consumption of GPU using the LRR and GTO warp scheduling algorithms normalized to the total register power consumed without compression. The average energy reduction with LRR is 26% which is very similar to the energy reduction with GTO (25%).

6.6. Design Space Exploration: Compression Parameters

Till now we assumed that the basic compression engine explores <4,0>, <4,1>, and <4,2> compression parameters and selects the parameter with the highest compression ratio with least number of required register bank accesses. In this section, we explore a simpler compression scheme that selects only one of the three choices statically. Such an implementation reduces the compression and decompression latencies and energy consumption, at the expense of missed opportunities for compression or unnecessary delta storages. For instance, when a register value could be compressed effectively with <4,1> then using <4,2> as the only compression choice leads to an additional byte of delta value for each 4-byte chunk. In addition, <4,0> correspond to scalarizing input operands [33], because <4,0> compression essentially captures those scenarios where all 32 thread register values are identical. Thus an
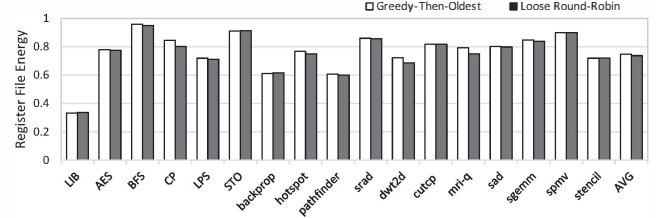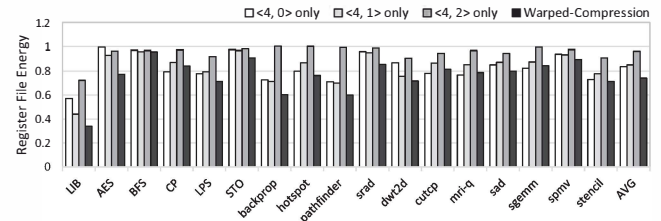
implementation that selects only <4,0> allows us to quantify the benefits of our proposed scheme compared to the scalarization approach [33] in terms of compression ratio and energy benefits.

Figure 15 shows the compression ratios seen when using only one set of compression parameters. The baseline is labeled as *Warped-Compression* in the figure. The compression ratio of <4,0> is about 30% less than the warped-compression scheme which selects one of the three choices dynamically. Note that while <4,1> can compress every register that was compressed with <4,0> it does not necessarily mean <4,1> has better compression ratio since an extra byte is stored for each chunk in this case. Thus it is possible that selecting just <4,1> has worse compression ratio than selecting just <4,0>, as was the case in a few benchmarks. Since the compression ratio of <4,0> is about 30% worse than warped-compression, as shown in Figure 16 the dynamic energy consumed by <4,0> is worse than the dynamic energy consumed using the warped-compression scheme.

6.7. Design Space Exploration: Access Energy Variations

In this section, we show the impact of increasing the compression and decompression unit activation energy by 1.5×, 2× and 2.5× the baseline energy data shown in Table 3. Figure 17 shows the register file energy consumption using three different compression and decompression unit activation energy values. The bar labeled 1.5× shows the total register file energy consumed when compression and decompression both take 1.5× the unit activation energy normalized to a design that does not use compression. Similarly 2.0×, 2.5× show the case when compression and decompression unit activation energies were increased by 2.0× and 2.5× over the baseline data shown in Table 3. For this data the register file access energy was kept same as the data shown in Table 3. Thus this data is a pessimistic view of the compression approach where
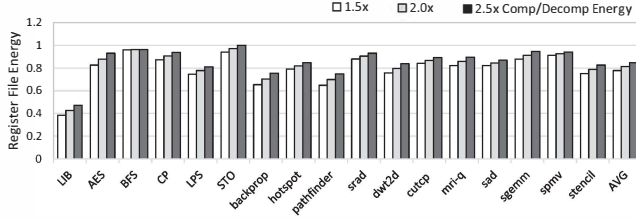
Figure 17: Energy consumption for various compression/decompression unit activation energy
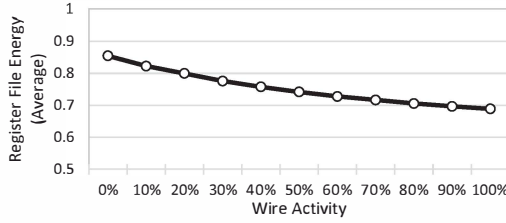

Figure 18: Energy consumption for various per-bank access energy

Figure 19: Impact of wire activity

the compression and decompression unit activation energy is significantly increased but the register access energy was kept the same. This scenario models the assumption that wire delays will not be the dominant factor in energy consumption, but logic computations will be the energy bottlenecks. As can be seen under such strong pessimistic assumptions the compression scheme saves 14% of the total register file energy in the worst scenario ($2.5\times$ Comp/Decomp Energy), compared to 25% register file energy savings seen in the base warped-compression implementation.

Figure 18 shows the total register file energy consumption for three different register file access energy values. For this data the compression and decompression unit activation energy was kept the same as shown in Table 3. But the register file access energy was increased by $1.5\times$, $2\times$ and $2.5\times$ in each bar shown in the figure. Thus this data is an optimistic view of the compression approach where the compression and decompression energy is unaltered but the register access energy was increased. This scenario models the assumption that wire delays and data movement on wires will in fact be the dominant factor in energy consumption, but logic computations will not be the energy bottlenecks. Under optimistic assumptions the warped-compression scheme saves 35% of the total register file energy compared with no register compression.

Figure 19 shows the register file energy consumption for various wire activity factors. We define wire activity as the fraction of wires connected to a 128-bit wide register bank that experience bit state change. In this experiment, we assume the energy values for register bank access and compression/decompression unit activation are same as shown in Table 3, and we only varied the wire activity from 0% to 100%. The energy value shown here is the average of all benchmarks. As discussed in Section 6.1, the wire energy contributes to a significant fraction of the register bank access energy, therefore the total register access energy increases as wire activity
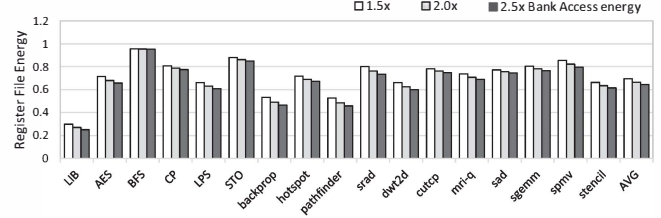
increases. When wire activity increases compression delivers higher energy savings, since fewer bits are moved across the wires. Thus when the wire activity increases to 100%, warped-compression can save 31% of the total register file energy.

6.8. Design Space Exploration: Latency Variations

In this section, we show the impact of increasing the compression and decompression latency on the overall performance. Figure 20 and Figure 21 shows the impact of changing the latency for compression to 2, 4, 8 and decompression to 2, 4, 8 cycles, respectively. Note that in our default settings compression takes two cycles while decompression takes one cycle. The data shows the execution time increase normalized to the baseline with no compression. On average increasing the compression and decompression latency in the worst case to 8 cycles increases the execution time by 14%.

7. Related Work

Register file power consumption has been addressed in several prior studies in both CPUs and GPUs. In general-purpose processors, prior studies focused on the partial activity in registers. Bit-partitioned register file [32] relies on the fact that many operands do not need the full bit width registers. Register file partitioning [25] employed circuit-level and compiler-level register partitioning techniques for reducing power of unused registers. Bypass-aware instruction scheduling [39] showed reductions in the register file power consumption can be obtained by reordering instruction schedules. Content-aware integer register file [24] exploits partial value locality on integer data values and represent data using three types of sub register files.

In case of the GPUs, several studies showed the register file as one of the critical power consuming component on GPU [35, 36]. Register file cache [21] employed hierarchical register file structure. This approach uses a small register cache to capture short-lived values on the main register file of GPU, and the register file cache filters a large number of access requests on the main register file and reduces dynamic power consumption. Circuit-level power reduction techniques are also adopted to reduce leakage power of the GPU register file. Using low power drowsy mode greatly reduces leakage power consumption with low wake-up penalty [9]. Active mask aware gating scheme exploits the SIMT execution char-
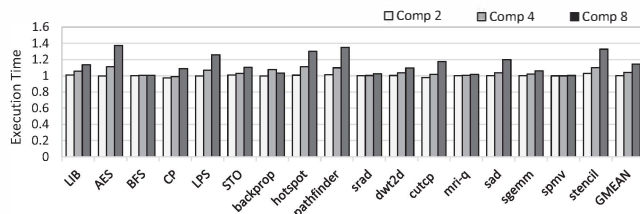
Figure 20: Execution time variation with increased compression latency

Figure 21: Execution time variation with increased decompression latency

acteristic of GPU to remove unnecessary register activity and helps to reduce the dynamic power [48].

Register compression is an orthogonal approach that tries to reduce power by exploiting the register value similarity property. Scalar unit [23, 15, 49] exploits a special case of value similarity where all thread registers of a warp register have the same value. Scalar register file [23] eliminates redundant power consumption in that case by storing the thread register value of only one SIMT lane shared across all lanes. Prior works [16, 17, 30, 33] have also used the notion of value similarity. Value structure [16] is exploited for improving memory storage efficiency [17] and power efficient computations [30]. However, they did not exploit value structure for improving register file efficiency, which is the primary focus of this paper.

Other studies reduce register file power by means of power-efficient memory cells such as embedded DRAM [28]. A hybrid register file was proposed which combines power-intensive SRAM register file and a large eDRAM register file [50]. The authors also proposed a context-aware scheduling that tries to give preference to warps whose registers are already brought into the SRAM register file. But our proposed design does not place any restriction on the warp scheduling algorithms.

Data compression on computer systems were proposed for improving performance of processor by saving memory bandwidth at various levels of the memory hierarchy [10, 40, 51, 14, 43, 46, 44]. In memory systems, data compression techniques significantly reduce bandwidth demands and channel energy consumed on data transfer. Therefore, data compression is widely used in commercial systems, especially on GPUs [6]. Cache compression techniques reduce the stored data size in the last level cache memory, therefore the effective size of cache memory is enlarged and cache hit ratio is also improved. However, implementing compression algorithm can add latency because they increases cache access and cache fill latency. Since CPUs are more latency sensitive, cache compression studies were typically applied to lower level caches that are latency tolerant. Base-Immediate-Delta compression algorithm [40] addressed the latency problem of cache compression algorithm by analyzing cache data similarity. However, the original BDI algorithm was primarily applied to cache designs and we adapted it to compress register files while working within the microarchitecture limitations of GPUs.
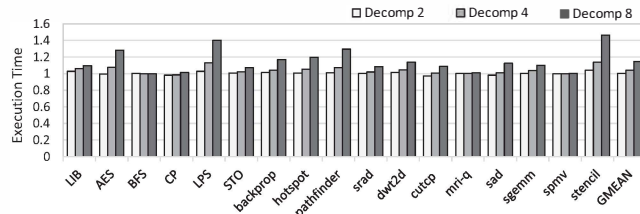
8. Conclusion

In this paper, we propose warped-compression, a register compression scheme for GPUs to save dynamic and leakage power. By reducing the number of register banks needed to store (and subsequently read) warp registers, the energy required to access register file is reduced. In addition, we applied simple power-gating to gate each register bank when none of the bank entries are allocated for a register. We provided solutions to deal with branch divergence. We did a thorough design space exploration to show that the proposed scheme is attractive over a wide range of technology parameter values.

Acknowledgements

References

[1] CACTI: An integrated cache and memory access time, cycle time, area, leakage, and dynamic power model. [Online]. Available: http://www.hpl.hp.com/research/cacti/

[2] FreePDK Process Design Kit. [Online]. Available: http://www.eda.ncsu.edu/wiki/FreePDK

[3] NVIDIA, CUDA C Programming Guide.

[4] NVIDIA, OpenCL Programming Guide.

[5] Parboil Benchmarks. [Online]. Available: http://impact.crhc.illinois.edu/Parboil/parboil.aspx

[6] Whitepaper: NVIDIA GeForce GTX 980.

[7] Whitepaper: NVIDIAs Next Generation CUDA Compute Architecture: Fermi.

[8] Whitepaper: NVIDIAs Next Generation CUDA Compute Architecture: Kepler GK110.

[9] M. Abdel-Majeed and M. Annavaram, "Warped Register File: A Power Efficient Register File for GPGPUs," in *Proceedings of the 2013 IEEE 19th International Symposium on High Performance Computer Architecture*, 2013, pp. 412–423.

[10] A. R. Alameldeen and D. A. Wood, "Adaptive Cache Compression for High-Performance Processors," in *Proceedings of the 31st Annual International Symposium on Computer Architecture*, 2004.

[11] A. Arelakis and P. Stenstrom, "SC2: A Statistical Compression Cache Scheme," in *Proceedings of the 41st Annual International Symposium on Computer Architecuture*, 2014, pp. 145–156.

[12] A. Bakhoda, G. Yuan, W. Fung, H. Wong, and T. Aamodt, "Analyzing CUDA Workloads Using a Detailed GPU Simulator," in *Proceedings of IEEE Int'l Symp. Performance Analysis of Systems and Software*, 2009, pp. 163–174.

[13] S. Che, M. Boyer, J. Meng, D. Tarjan, J. Sheaffer, S.-H. Lee, and K. Skadron, "Rodinia: A Benchmark Suite for Heterogeneous Computing," in *Proceedings of IEEE International Symposium on Workload Characterization*, 2009, pp. 44–54.

[14] X. Chen, L. Yang, R. P. Dick, L. Shang, and H. Lekatsas, "C-pack: A High-performance Microprocessor Cache Compression Algorithm," *IEEE Trans. Very Large Scale Integr. Syst.*, vol. 18, no. 8, pp. 1196–1208, Aug. 2010.

[15] Z. Chen, D. Kaeli, and N. Rubin, "Characterizing scalar opportunities in GPGPU applications," in *Proceedings of the 2013 IEEE International Symposium on Performance Analysis of Systems and Software*, 2013, pp. 225–234.

[16] S. Collange, D. Defour, and Y. Zhang, "Dynamic Detection of Uniform and Affine Vectors in GPGPU Computations," in *Euro-Par 2009 - Parallel Processing Workshops*, ser. Lecture Notes in Computer Science. Springer Berlin Heidelberg, 2010, vol. 6043, pp. 46–55.

[17] S. Collange and A. Kouyoumdjian, "Affine Vector Cache for memory bandwidth savings," Universite de Lyon, Tech. Rep., 2011.

[18] B. Dally, "The Future of GPU Computing," in *Proceedings of the 22nd Annual Supercomputing Conference*, 2009.

[19] L. P. Deutsch, "DEFLATE Compressed Data Format Specification Version 1.3," 1996.

[20] W. Dweik, M. Abdel-Majeed, and M. Annavaram, "Warped-Shield: Tolerating Hard Faults in GPGPUs," in *Proceedings of the 2014 44th Annual IEEE/IFIP International Conference on Dependable Systems and Networks*, 2014, pp. 431–442.

[21] M. Gebhart, D. Johnson, D. Tarjan, S. Keckler, W. Dally, E. Lindholm, and K. Skadron, "Energy-efficient Mechanisms for Managing Thread Context in Throughput Processors," in *Proceedings of the 38th Annual International Symposium on Computer Architecture*, 2011, pp. 235–246.

[22] M. Gebhart, S. W. Keckler, and W. J. Dally, "A Compile-time Managed Multi-level Register File Hierarchy," in *Proceedings of the 44th Annual IEEE/ACM International Symposium on Microarchitecture*, 2011, pp. 465–476.

[23] S. Gilani, N. S. Kim, and M. Schulte, "Power-efficient computing for compute-intensive GPGPU applications," in *Proceedings of the IEEE 19th International Symposium on High Performance Computer Architecture*, 2013, pp. 330–341.

[24] R. Gonzalez, A. Cristal, D. Ortega, A. Veidenbaum, and M. Valero, "A Content Aware Integer Register File Organization," in *Proceedings of the 31st Annual International Symposium on Computer Architecture*, 2004, pp. 314–324.

[25] X. Guan and Y. Fei, "Register File Partitioning and Recompilation for Register File Power Reduction," *ACM Trans. Des. Autom. Electron. Syst.*, vol. 15, no. 3, pp. 24:1–24:30, Jun. 2010.

[26] P. Hammarlund, A. Martinez, A. Bajwa, D. Hill, E. Hallnor, H. Jiang, M. Dixon, M. Derr, M. Hunsaker, R. Kumar, R. Osborne, R. Rajwar, R. Singhal, R. D'Sa, R. Chappell, S. Kaushik, S. Chennupaty, S. Jourdan, S. Gunther, T. Piazza, and T. Burton, "Haswell: The Fourth-Generation Intel Core Processor," *IEEE Micro*, vol. 34, no. 2, pp. 6–20, Mar 2014.

[27] H. Jeon and M. Annavaram, "Warped-DMR: Light-weight Error Detection for GPGPU," in *Proceedings of the 2012 45th Annual IEEE/ACM International Symposium on Microarchitecture*, 2012, pp. 37–47.

[28] N. Jing, Y. Shen, Y. Lu, S. Ganapathy, Z. Mao, M. Guo, R. Canal, and X. Liang, "An Energy-efficient and Scalable eDRAM-based Register File Architecture for GPGPU," in *Proceedings of the 40th Annual International Symposium on Computer Architecture*, 2013, pp. 344–355.

[29] S. W. Keckler, W. J. Dally, B. Khailany, M. Garland, and D. Glasco, "GPUs and the Future of Parallel Computing," *IEEE Micro*, vol. 31, no. 5, pp. 7–17, 2011.

[30] J. Kim, C. Torng, S. Srinath, D. Lockhart, and C. Batten, "Microarchitectural Mechanisms to Exploit Value Structure in SIMT Architectures," in *Proceedings of the 40th Annual International Symposium on Computer Architecture*, 2013, pp. 130–141.

[31] P. Kogge, K. Bergman, S. Borkar, D. Campbell, W. Carson, W. Dally, M. Denneau, P. Franzon, W. Harrod, K. Hill *et al.*, "Exascale Computing Study: Technology Challenges in Achieving Exascale Systems," 2008.

[32] M. Kondo and H. Nakamura, "A small, Fast and Low-power Register File by Bit-partitioning," in *Proceedings of the 11th International Symposium on High-Performance Computer Architecture*, 2005, pp. 40–49.

[33] Y. Lee, R. Krashinsky, V. Grover, S. Keckler, and K. Asanovic, "Convergence and scalarization for data-parallel architectures," in *Proceedings of the 2013 IEEE/ACM International Symposium on Code Generation and Optimization*, 2013, pp. 1–11.

[34] C. Lefurgy, P. Bird, I.-C. Chen, and T. Mudge, "Improving Code Density Using Compression Techniques," in *Proceedings of the 30th Annual IEEE/ACM International Symposium on Microarchitecture*, 1997, pp. 194–203.

[35] J. Leng, T. Hetherington, A. ElTantawy, S. Gilani, N. S. Kim, T. M. Aamodt, and V. J. Reddi, "GPUWattch: Enabling Energy Optimizations in GPGPUs," in *Proceedings of the 40th Annual International Symposium on Computer Architecture*, 2013, pp. 487–498.

[36] J. Lucas, S. Lal, M. Andersch, M. Alvarez-Mesa, and B. Juurlink, "How a Single Chip Causes Massive Power Bills GPUSimPow: A GPGPU Power Simulator," in *Proceedings of the 2013 IEEE International Symposium on Performance Analysis of Systems and Software*, 2013, pp. 97–106.

[37] S. Molnar, B. Schneider, J. Montrym, J. Van Dyke, and S. Lew, "System and Method for Real-time Compression of Pixel Colors," Nov. 30 2004, uS Patent 6,825,847.

[38] M. R. Nelson, "LZW Data Compression," *Dr. Dobb's Journal*, vol. 14, no. 10, pp. 29–36, 1989.

[39] S. Park, A. Shrivastava, N. Dutt, A. Nicolau, Y. Paek, and E. Earlie, "Bypass Aware Instruction Scheduling for Register File Power Reduction," in *Proceedings of the 2006 ACM SIGPLAN/SIGBED Conference on Language, Compilers, and Tool Support for Embedded Systems*, 2006, pp. 173–181.

[40] G. Pekhimenko, V. Seshadri, O. Mutlu, P. B. Gibbons, M. A. Kozuch, and T. C. Mowry, "Base-Delta-Immediate Compression: Practical Data Compression for On-chip Caches," in *Proceedings of the 21st International Conference on Parallel Architectures and Compilation Techniques*, 2012, pp. 377–388.

[41] T. Rogers, M. O'Connor, and T. Aamodt, "Cache-Conscious Wavefront Scheduling," in *Proceedings of the 2012 45th Annual IEEE/ACM International Symposium on Microarchitecture*, 2012, pp. 72–83.

[42] K. Sankaralingam, R. Nagarajan, H. Liu, C. Kim, J. Huh, D. Burger, S. W. Keckler, and C. R. Moore, "Exploiting ILP, TLP, and DLP with the Polymorphous TRIPS Architecture," in *Proceedings of the 30th Annual International Symposium on Computer Architecture*, 2003, pp. 422–433.

[43] S. Sardashti and D. Wood, "Decoupled Compressed Cache: Exploiting Spatial Locality for Energy Optimization," *IEEE Micro*, vol. 34, no. 3, pp. 91–99, May 2014.

[44] V. Sathish, M. J. Schulte, and N. S. Kim, "Lossless and Lossy Memory I/O Link Compression for Improving Performance of GPGPU Workloads," in *Proceedings of the 21st International Conference on Parallel Architectures and Compilation Techniques*, 2012, pp. 325–334.

[45] Y. Sazeides and J. Smith, "The Predictability of Data Values," in *Proceedings of the 30th Annual IEEE/ACM International Symposium on Microarchitecture*, 1997, pp. 248–258.

[46] A. Shafiee, M. Taassori, R. Balasubramonian, and A. Davis, "MemZip: Exploring unconventional benefits from memory compression," in *Proceedings of the 2014 IEEE 20th International Symposium on High Performance Computer Architecture*, 2014, pp. 638–649.

[47] A. T. Tran and B. M. Baas, "Design of an Energy-efficient 32-bit Adder Operating at Subthreshold Voltages in 45-nm CMOS," in *Proceedings of the 2010 Third International Conference on Communications and Electronics*. IEEE, 2010, pp. 87–91.

[48] Q. Xu and M. Annavaram, "PATS: Pattern Aware Scheduling and Power Gating for GPGPUs," in *Proceedings of the 23rd International Conference on Parallel Architectures and Compilation*, 2014, pp. 225–236.

[49] Y. Yang, P. Xiang, M. Mantor, N. Rubin, L. Hsu, Q. Dong, and H. Zhou, "A Case for a Flexible Scalar Unit in SIMT Architecture," in *Proceedings of the 2014 IEEE 28th International Parallel and Distributed Processing Symposium*, 2014, pp. 93–102.

[50] W.-k. S. Yu, R. Huang, S. Q. Xu, S.-E. Wang, E. Kan, and G. E. Suh, "SRAM-DRAM Hybrid Memory with Applications to Efficient Register Files in Fine-grained Multi-threading," in *Proceedings of the 38th Annual International Symposium on Computer Architecture*, 2011, pp. 247–258.

[51] Y. Zhang, J. Yang, and R. Gupta, "Frequent Value Locality and Value-centric Data Cache Design," in *Proceedings of the 9th International Conference on Architectural Support for Programming Languages and Operating Systems*, 2000.